Journal of Applied Fluid Mechanics, Vol. 15, No. 6, pp. 1947-1955, 2022.
Available online at www.jafmonline.net, ISSN 1735-3572, EISSN 1735-3645.
https://doi.org/10.47176/jafm.15.06.1324

Experimental Investigation of Aluminum Oxide Nanofluid on Closed Loop Pulsating Heat Pipe Performance

P. Venkataramana[1]†, P. Vijayakumar[2] and B. Balakrishna [1]

[1] *JNTU College of Engineering, Kakinada, Department of Mechanical Engineering, Andhra Pradesh, 533003, India*
[2] *Lakireddy Balireddy College of Engineering, Department of Mechanical Engineering, Mylavaram, Andhra Pradesh,521320, India*

†Corresponding Author Email: venkataramana.me@srecnandyal.edu.in

(Received May 22, 2022; accepted July 30, 2022)

ABSTRACT

This paper discusses the experimental studies performed on a single closed loop pulsating heat pipe (CLPHP) to evaluate its thermal performance. The pulsating heat pipe is brass which has a single closed loop. Aluminium oxide (Al_2O_3) and deionized (DI) water nanofluid were utilized as working fluids, with different volume concentrations of aluminium oxide nanoparticles of 0.05 %, 0.5 % and 1%. The aluminium oxide particles are mixed with water in the two-step method to produce a stable suspension. Experiments are carried out in the horizontal mode with watt loads of heat inputs ranging from 10 w to 100 w. The temperature differences between the evaporator and condenser portions, thermal resistance, heat transfer coefficient and thermal conductivity are the parameters used to determine thermal performance. The thermal resistance of aluminium oxide and DI water nanofluid was the lowest, having 48 % less than that of water. The effective thermal conductivity of the heat pipe improves as the concentration of nanoparticles increases. The comparison between experimental results and computational fluid dynamics (CFD) simulation results CLPHP was carried out under the same condition.

Keywords: Nanofluid; Pulsating heat pipe; Adiabatic section; Thermo-hydrodynamic; Working fluid.

NOMENCLATURE

A	surface area of condenser	Al_2O_3	aluminum oxide
t	time	C	compressor
ρ_1	density of liquid	$CLPHP$	Closed Loop Pulsating Heat Pipe
ρ_2	density of Vapour		

1. INTRODUCTION

With the fast expansion of the information and aeronautics sectors, small-volume, high-efficiency heat transfer equipment is required. Micro PHP technology has advanced through multiple stages in recent years. A pulsating heat pipe serves as a cooling device. Akachi (1990), a Japanese scientist, suggested the PHP as just a novel sort of heat pipe. Since PHP's inception, the operating mechanism and heat transmission properties have been extensively investigated. PHP's functioning mechanism is complex Khandekar *et al*. (2003). The working fluid is heated in the evaporator portion, and its volume expands fast, creating bubbles. When it enters the condenser portion, the volume rapidly reduces. When an internal phase shift occurs, the working fluid is flowing continually from the E to the C portion, then back to the E after condensation, establishing a directed circulating flow.

The working fluid flows whenever the internal phase changes. The PHP's operation is based on the oscillation of the operating liquid and phase variations inside the pulsing heat pipe. The pulsing heat pipe is a natural-powered device that uses just the energy obtainable from the heat source and does not require any extra electricity. Khadekar (2004) suggested that, PHP is referred as a passive cooling device. For effective heat transmission between evaporator and condenser portions, the working fluid's latent and sensible heat portions are properly assessed.

PHPs are offered in two different designs:

- Closed end pulsating heat pipe (CEPHP)
- Closed loop PHP [CLPHP)

While various techniques are available, the CLPHP is the most often used. The CLPHP's success may be attributed to its cost-effective yet straightforward construction, simplicity of production, and high heat transfer rates. Mohammadi *et al*. (2013). The PHP is best suited for cooling electrical equipment as a heat transfer device. However, in current centuries, pulsating heat pipes have initiated use in various applications, including air heating, radiators for interrestrial and terrestrial refrigeration, waste heat retrieval, condensers for vapour compression refrigeration, cooling of fuel cells and heat exchangers Markal *et al*. (2021).

Ji *et al*. (2011) investigated the influence of nanoparticle shape on pulsating heat pipe transmission performance. The base fluid was a dual combination of H_2O and ethanol of equal volume. Four distinct aluminium nanoparticles were used: platelet, cylindrical, blade and brick. According to the findings, nanoparticles with cylindrical forms perform the best related to the supplementary types. They determined that particle volume segment also adds to heat transmission increase and particle shape. Karthikeyan *et al*. (2014) used nanofluids to conduct experimental tests on the heat transfer enactment of a closed-loop pulsating heat pipe. They discovered that using nanofluids improved heat transfer performance by 33 per cent compared to the primary fluid.

An experimental investigation on one-turn closed-loop PHP was reported by Rama Narashima *et al*. (2012). For various working fluids, heat input and evacuation levels, transient and steady-state studies were performed. According to the authors, the saturation temperature of the working fluid is greater under atmospheric conditions than in evacuated scenarios. As a result, more liquid exits in the PHP tube below the heat input range of 15 w, resulting in increased heat transmission. Their investigations revealed an intermittent motion of the working fluid with decreased heat input.

Wang *et al*. (2021) use Al_2O_3 water nanofluids as working fluids to examine the thermal performance of a heat pipe. It is concluded that, when loaded with a 3% concentration of Al_2O_3 water nanofluid, the thermal resistance dropped by 40% compared to DI water. The development of nano-covering on the heat pipes evaporator portion enhances thermal performance. Zhou *et al*. (2021) investigated screen mesh wick heat pipes utilizing Al_2O_3-DI water nanofluids as working fluids. Al_2O_3-DI water nanofluids are used as working fluids in an experimental investigation on wick PHP. The nanoparticles were chosen in the range of 100 to 200 nanometers. The heat transfer performance of the PHP were studied at two distinct percentages mass attentions a cyclic rise and reduction in Q input to the heat pipe's evaporator portion.

According to the literature review, while different type's nanofluids are utilized in further research to evaluate the pulsating heat pipe performance, no study has so far reported the pulsating heat pipe performance built of brass with aluminium oxide nanofluid and DI water. As a result, the current experiment investigates the thermal performance of a single closed loop PHP employing aluminium oxide (Al_2O_3) and DI water as the working fluid.

2. EXPERIMENTAL SETUP

The experimental work was restricted to measuring temperatures in PHP. It understands the flow arrangements and temperature variations in a pulsating heat pipe. PHP's heat efficiency requires to be studied below the impact of flow patterns and changes in temperature. Therefore, the research on thermo-hydrodynamic conduct of single loop pulsating heat pipe is more important to the current research. PHP's performance under the impact of evacuation requires to be studied. It is essential to evaluate the pulsating movement of the fluid in a PHP while developing the current experimental configuration, and there will be no leakage of the working fluid. The PHP of a single turn is produced in the experimental setup, and the unit has functioned with vacuum circumstances and a cooling water arrangement. Under the transient experiments, evaluated working temperatures and chilling liquid flow rates. The experiments are performed for distinct heat inputs working liquids and varying rate evacuation.

Figure 1 demonstrates the pictorial perspective of the experimental configuration created for heat transfer research. Silicon rubber tube, filling valve, Brass tube, wire heater, and type K thermocouples are the major apparatuses utilized in the pulsing heat pipe preparation. The characteristics such as elevated bending ease into curved forms, lower price, corrosive resistance, compatibility with most working liquids and excellent thermal conductivity give an additional advantage for brass over the other pipe components. The selected brass pipe's ID is 2 mm, and the OD is 3mm Rao *et al*. (2016). The glass tube is regarded as an adiabatic section with the evaporator section and condenser section U-turns. The clear surface of the glass tube may catch visual steam impacts. However, up to 1000 ℃ the glass tube's temperature resistance is high. Brass and glass tubes are coupled to silicon rubber connectors. There are evidence of leakage and grow at greater temperatures. The heating capability wire heater up to 100 watts winded over the portion of the evaporator and acts as the heat source. Eight thermocouples, four in the evaporator section and reminders in the condenser section, are connected for temperature measurement. The temperature information was registered at a frequency of 1 Hz using an eight-channel MCC USB-TC. Conducted the experiments with working liquids that are aluminium oxide - DI water nanofluid. A needle inserted liquid through a substantial controller during each operating cycle.

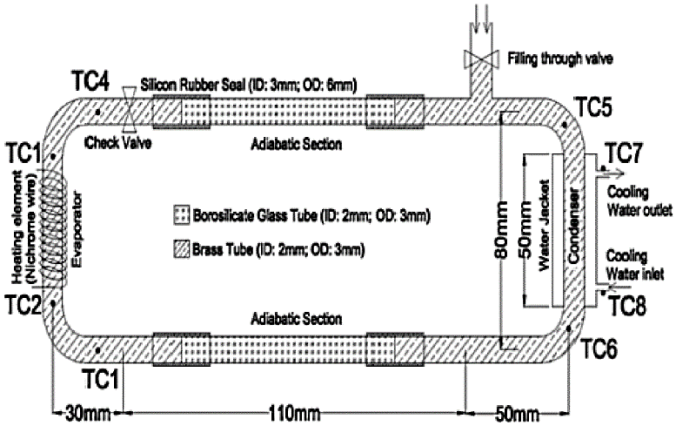

Fig. 1. Experimental Setup.

2.1 Preparation of Nanofluid

Nanofluids have been shown conjointly conceptual and experimentally to be superior heat transfer liquids when related to base fluids, and they are being used in thermal exchange systems for a wide range of industrial and medical use. They are two different approaches for preparing nanofluids: one step and two-step methods Sandhya *et al*. (2021). The nanoparticles are created and dispersed in the liquid instantaneously in one step method. The dried nanoparticles were distributed addicted to a stable fluid host in a two-step method.

In this work, Al_2O_3 nanoparticles were chosen as the source material, while DI water was employed as the base fluid. The water based nanofluids were created in two step method according to Parthasarathi *et al*. (2021). In the first step Al_2O_3 nanoparticles and DI water mixed in direct mixing process. In the second step, after creating surfactant mixture by suspending nanoparticles in base fluid and changing the pH valve of the suspension while it is maintained under ultrasonic vibration for six hours. Finally, Al_2O_3-water nanofluids have been prepared and the process is represented in flowchart as shown in Fig. 2. Hence, this process is simple to make and chemically stable in base fluids.

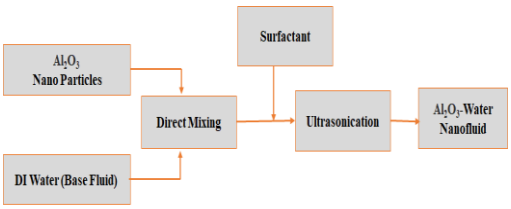

Fig. 2. Two-step method.

Improving nanofluid thermophysical properties validates their usage in heat transfer Stalin *et al*. (2021). However, the collected works show an ambiguous image of declaring the amount of fluctuation in the thermophysical characteristics of nanofluids with modification in volume concentration, temperature, nanoparticle size form, and base fluid, natural features. The literature reveals that these factors have a considerable effect on the thermal conductivity of nanofluids and are discussed in depth individually. The literature supplied by different scholars is represented, and the results are analyzed to understand the influence of individual characteristics. The aluminium oxide nanoparticles properties and Deionized water (DI) properties (as received) are illustrated in Table 1 and Table 2.

Table 1 Aluminium oxide nanoparticles properties

Property	Aluminium oxide nanoparticles
Thermal Conductivity	39 W/m K
Specific Heat	0.774 J / g K
Density	3780 Kg/m^3
Exact surface	14-18 m^2/g
Expansion Coefficient	5.3 X 10 ^ 6 m/k
Enthalpy	10 j/g
Hardness	1500-200

Table 2 Properties of Deionized water

Property	DI water
Melting point	0 ° C
Boiling point	100 ° C
Molar mass	17.01 gm./mole
Thermal conductivity	0.6158 W/mK
Density	999.98 Kg/m3
Viscosity	0.89 cp
Specific heat capacity	74.537 J/mole k
Acidity	13.995

2.2 Experimental Procedure

It is assured that there is no fluid with in the tubes prior to beginning the experiment. The required volume of working fluid is then injected with a syringe by opening one end of the non-return valve, allowing the fluid to reach the evaporator portion directly. Another syringe is now used to fill the air via the opening of the brass tube. This is done to assure the formation of a liquid slug and a vapour plug at the same time. The display device is turned

ON, and the necessary wattage is set. The fluid in the condenser portion is cooled using a cooling water supply. The transient tests are carried out, and the temperature data logger is used to record the varied temperatures. The experiments are carried out until a stable state is attained.

2.3 Uncertainty analysis

Heat input to the heat source is used to evaluate the operating constraints of the heat pipe and the temperature spreading throughout the pulsating heat pipe, and the thermal resistance at increasing heat loads ranging from 10 to 100 watts is determined using deionized H_2O and varying quantities of nanofluids, i.e. 0.05 %, 0.5 % and 1 % volume. Eq.1 is often used to calculate the heat input to the evaporator portion, where Cp is the specific heat.

$$Q_{input} = mC_p\Delta t \tag{1}$$

Eq. 2 is used to compute the total thermal resistance (R th) of the heat pipe, where Tae, Tac and Q input signify the average evaporator, condenser temperatures and heat input.

$$R_{th} = \frac{(Tae - Tac)}{Q_{input}} \tag{2}$$

The heat transfer rate expresses the quantity of heat transfer (h) rate between a liquid and the wall over which the fluid flows. Pradeep *et al*. (2019). A high heat transfer coefficient is recommended for improved performance.

$$h = \frac{Q_{input}}{A(Tae - Tac)} \tag{3}$$

Fluid thermal conductivity (K) values of aluminium oxide / water based nanofluid measured using various approaches. For the most part Fourier's law has been employed to calculate thermal conductivity. Regardless of the technology used, the trend reveals that thermal conductivity increase with increasing volume fraction, where $\frac{dt}{dx}$ is the temperature gradient.

$$Q_{input} = -KA\frac{dt}{dx} \tag{4}$$

The experimental setup's reliability is proven by equating the Nusselt number (Nu) of base fluid 50:50 ratio (water: aluminium oxide) combination by Dittus and Boelter (1930) single phase liquid relation in Eq.5. Similar observations are made by Wu *et al*.

$$Nu = 0.023\,\mathrm{Re}^{0.8}\,\mathrm{Pr}^{0.4} \tag{5}$$

The temperature is monitored with K- type thermocouples and then transmitted to the data analysis, with an error of ± 2 % of full scale. The power supply voltage and current are both accurate to 0.1 percent. However, the heating power is set to 10 watts, respectively.

2.4 Governing Equation

The formation of liquid slug is the most crucial condition of PHP. Surface tension and buoyancy in the channel influence the appearance and movement of bubbles. The dimensionless formula presented in Eq. 6 might explain the relationship between surface tension and buoyancy.

$$E = g\left[\frac{D^2(\rho_1 - \rho_2)}{\sigma}\right] \tag{6}$$

3. SIMULATION OF CLPHP

Figure 3 shown the Geometry model of PHP. Because of the chaotic nature of the closed loop pulsating heat pipe (CLPHP), modelling the internal heat flow and heat transfer during pulsation is extremely difficult. According to a review of the literature, there is yet no mature model that accurately predicts the thermal performance of closed loop pulsating heat pipe. CFD simulation is required to investigate the behavior of CLPHP Yao *et al*. (2022). This work used the volume of the fluid model in transient mode to simulate the multiphase flow process of the closed-loop pulsating heat pipe and forecast the thermal performance of the closed-loop pulsating heat pipe in ANSYS FLUENT 15.0. There is also no mass interface between the closed-loop pulsating heat pipe and its surroundings.

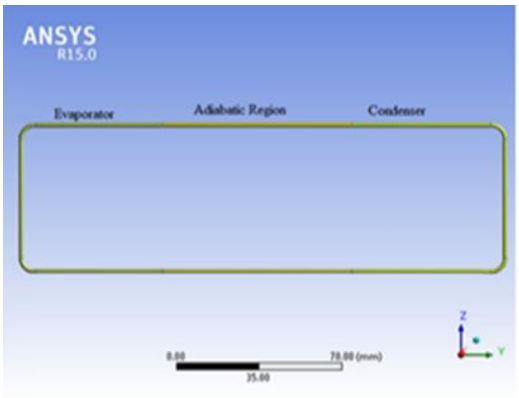

Fig. 3. Geometry model.

3.1 Meshing

ANSYS meshing gives more control over the automatic settings by allowing to define combinations point Grubisic *et al*. (2022), surface and body controls. Both of them has its individual set of parameters and may be used to modify the mesh in various ways. In this situation, the automated method for mesh shape is used, however, the mesh sizing is done. As demonstrated in Fig. 4, the least and extreme mesh sizes are set to 0.01 mm. Meshing is created using 2, 26,318 nodes and 3, 34,642 elements with control option is used. It is at the meshing stage that the portions of the geometry are given names, making it easier to define domains and specify boundary conditions in the CFX-PRE setup section.

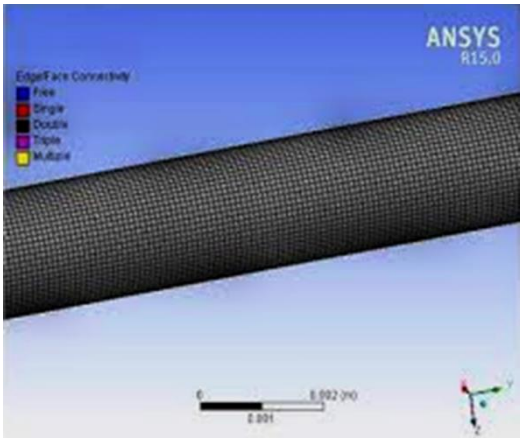

Fig. 4. Meshing in ANSYS.

3.2 Boundary Conditions

There was undesirable pressure within the tube because a vacuum was produced during the filling operation and the working fluid was filled. According to the experimental results, the boiling point of water was considered to be 298K. When the liquid phase temperature surpasses the saturation temperature, evaporation begins. Condensation happened when the temperature of the vapour phase fell below 298K.The power input determined the heat input in the evaporation portion. The heating powers employed in simulations are not greater than 90 watt. Because CLPHPs are made up of capillary tubes, surface tension has a significant impact. The continuum surface force model was employed in both situations to examine the influence of surface tension.

Different heat fluxes were given to the evaporator region; they are 10 W to 100 W. For the adiabatic region, heat flux is zero. In the condenser region, negative heat flux is given; this heat flux is in all domains, and walls are of no-slip wall types. All the walls are assumed to be smooth walls. The thermal boundary condition with a fixed temperature of 298 K is set in the condenser. Similarly, the boundary condition in adiabatic zones is adiabatic, defining the heat flux rate as 0 W/m^2 K. In the evaporator region, where the external heat source is attached, the total constant heat flux of value 1000 W/m^2 K.

Computational continuum mechanics (CCM+) separated solver was launched; because of the oscillation properties of CLPHPs Yoon and Kim (2021), chosen unstable time condition and implied gravitational enabled body forces and heat transmission by stimulating the energy equations. The viscous model was created using heating since vapour begins at boiling temperature; hence the boiling term is also reflected. The pressure velocity relationship in the model solution was straightforward. The liquid filling ratio is set at 50% from the start. The simulation tracked the temperature progression for at least 50 seconds. CLPHP was able to achieve a stable operation within this time frame.

3.3 Periphery Conditions

Heat fluxes of 10 to 16 watts have been provided to the evaporator portion, while the heat flux in the adiabatic portion is zero. In the condenser portion, a negative heat flux was reported, this heat flux was chosen on purpose based on references. For the computational fluid dynamics study, all the walls are considered to be smooth, with no slip in any domains, and a volume flow model is used Bai *et al.* (2022). The condenser section's thermal boundary conditions are adjusted at a static temperature of 298 k. Similarly, the boundary condition in adiabatic portion with the heat flow rate defining as zero W /m^{2}K.Total continuous heat flow of 6854 W /m^{2}K in the portion of the evaporator heat source is devoted.

4. RESULTS AND DISCUSSION

The thermal resistance (Eq. 2), heat transfer coefficient (h) (Eq. 3), and thermal conductivity (K) (Eq. 4) are the parameters used to evaluate the performance of a PHP. Thermal resistance and heat transfer coefficient values are affected by the average temperature difference between the evaporator and condenser (Tae-Tac). The rapid flow of the working fluid allows for effective heat transmission between the hot and cold ends in this situation. The heat transfer rate is significantly affected by the temperature build-up in the evaporator whenever the temperature difference between the evaporator and the condenser is significant. In an effective heat transfer process, low values of (Tae-Tac) are observed. In the existing study, the operational fluid with the lowest (Tae-Tac) values may be regarded as a superior heat transmission fluid.

The resistance of a PHP system to heat passage from the evaporator to the condenser is known as thermal resistance. It's also the difference in average temperatures between the evaporator and the condenser to the heat input (Eq. 2). The heat transfer coefficient (h) describes how much heat is transferred between a fluid and the wall it passes through (Eq. 3). For better performance, a high heat transfer coefficient is preferred. It has been discovered in studies involving nanofluids that the thermal conductivity of a nanofluid is mainly greater than that of base fluids.

(a) Effect of the temperature difference between evaporator and condenser (Tae–Tac)

The transient change of difference in temperature between the evaporator and condenser for various working fluid concentrations is shown in Fig. 5. It can see that the values of (Tae-Tac) for all working fluids exhibit a rising tendency over time. Heat may be carried from the evaporator to the condenser using any functioning fluidity. The (Tae-Tac) values for water are more significant than for other liquids, with the lowest value achieved for a 1 % aluminium (Al_2O_3) – DI water nanofluid. This discovery demonstrates that heat transmission is more efficient in Al_2O_3 – based nanofluids than in water. Although a 1 % Al_2O_3 nanofluid is heavier than H_2O (due to

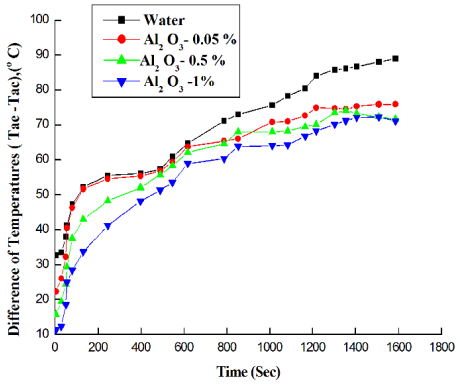

Fig. 5. Time Vs Difference of Temperature (Tae-Tac).

aluminium oxide nanoparticles in water), heat absorption causes fully randomized movements of the $Al_2 O_3$ particles inside the fluid. The thermal conductivity improvement of the nanofluid, as seen in all nanofluids, results in improved heat transmission. As a result, the most considerable temperature difference achieved is roughly 90°C. Heat transfer in pure water is regulated by latent and sensible heat, which are both constant, and there is no extra turbulence owing to the unavailability of nanoparticles.

(b) Effect of heat input (Q_{input}) on Thermal resistance (R_{th})

The variation of thermal resistance with heat input is shown in Fig. 6. As the Q_{input} growths from 10 to 100 watts, it appears that all fluids are verified to have a reducing tendency in thermal resistance. It may also indicate that the $Al_2 O_3$ 1 % -H_2O nanofluid has the lowermost thermal resistance of completely working fluids. The thermal resistance reduces as the Q_{input} growths from 10 to 100 watts. The lower thermal resistance might be attributed to the working fluid's improved heat transfer capabilities. The nanofluid, in conjunction with water, improves heat transfer capability.

(c) Heat input (Q_{input}) influence on heat transfer coefficient (h)

Figure 7 shows the fluctuation of heat transfer coefficients for various fluids at various heat inputs. The graph shows that the H increases as the Q_{input} increases from 10 to 100 watts. The maximum h recorded among all fluids is for the $Al_2 O_3$ 1 % – water nanofluid, which is close to 850 W/m^2 °C. This might similarly be related to the nanofluid's improved thermal characteristics, such as K, as compared to pure water.

(d) Effect of Q_{input} on thermal conductivity (K)

Figure 8 demonstrates that the thermal conductivity values obtained for all heat sources are substantially lower than those found for the $Al_2 O_3$ 1% –water nanofluid. The thermal conductivity values determined for the fluids $Al_2 O_3$ -1 %, 0.5 %, 0.05 % and DI water with a heat input of 10 to 100 watts. As a result, the trend of increasing thermal conductivity with increasing nanoparticle concentration can be observed.

(e) Validation of based fluid

Experiments with base fluid and $Al_2 O_3$ nanofluid at volume concentrations of 0.05 %, 0.5 % and 1 % at varying flow rates are shown in Fig. 9. The number of nanoparticles floating in the base fluid increases, as does the Nusselt number. This pattern was discovered by Singh *et al.* (2021), who noted the large increase in Nusselt number owing to an increase in thermal conductivity. As a result, a greater Nusselt number indicates that the convection process is more efficient. According to Rahman and Saghir (2021), such increases are influenced by suspended particles near the wall, boundary layer decreases, which is supported by Xilong Zhang *et al.* (2021). The average Nusselt number of 1 Vol.% nanofluid was enhanced by 28 % as compare to pure water due to temperature differences of (Tae-Tac).

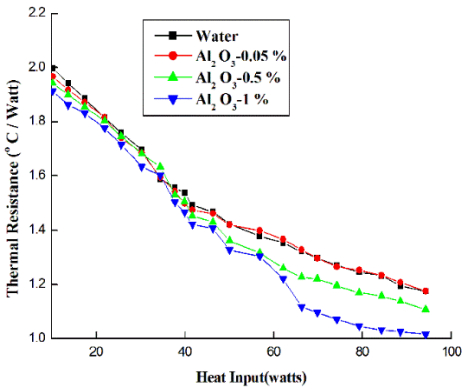

Fig. 6. Heat Input Vs Thermal Resistance.

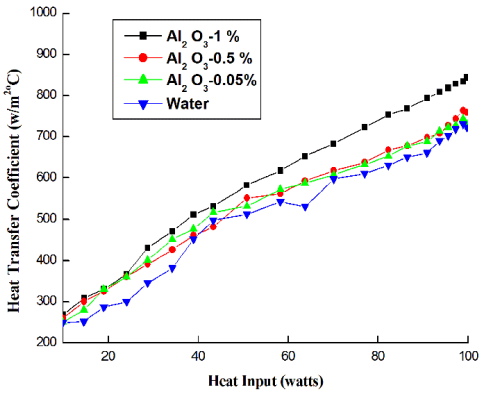

Fig. 7. Heat Input Vs Heat transfer coefficient.

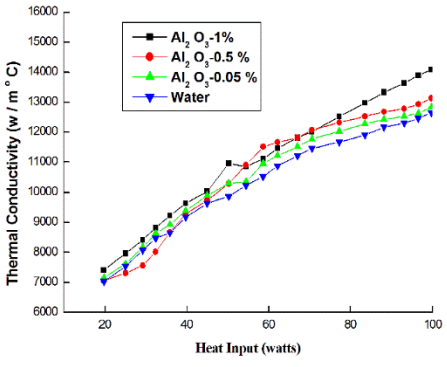

Fig. 8. Heat Input Vs Thermal Conductivity.

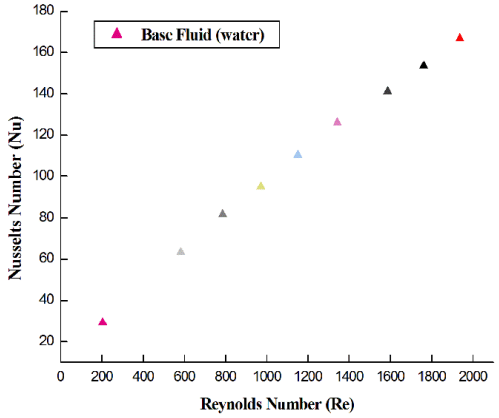

Fig. 9. Reynolds Number Vs Nusselt Number.

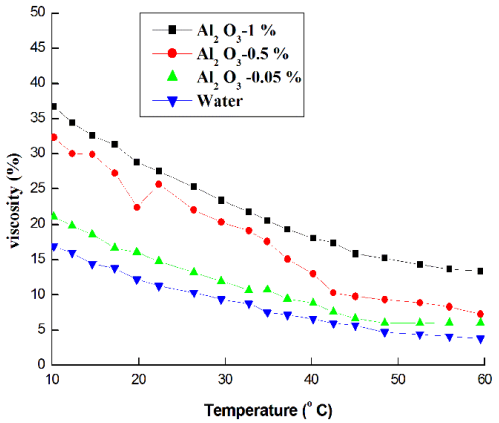

Fig. 10. Temperature Vs viscosity.

Figure 10 illustrates the viscosity behavior of the nanofluids in comparison to viscosity of base fluids under the identical measurement circumstances. The fluctuation of the nanofluids viscosity with temperature is logarithmic, indicating that the nanofluids follow an Arrhenius-type relationship, and the results is consistent with the literature. The nanofluids' viscosity decreases gradually with increasing temperature. The dependency of viscosity on temperature of the nanofluids, on the other hand, is more prominent at 1 % particle loading. This might indicate that the contribution of particle interactions to the increase in viscosity of nanofluids is stronger at lower temperatures and fades when the energy of Brownian movements owing to temperature.

4.1 Simulation Results

The simulation results may be displayed in numerous ways, including contours, charts and graphs; different parameter values are monitored and shown as contours. The temperature of the pulsating heat pipe at the section of the E and C are plotted to provide clear images from Fig. 11 and Fig. 12, and simulation findings may be evaluated by looking at these contours. The volume of the working fluid would alternately circulate from the outlines in vapour bubbles, emerging in nearby channels and achieving steady oscillation. At low heat input, did

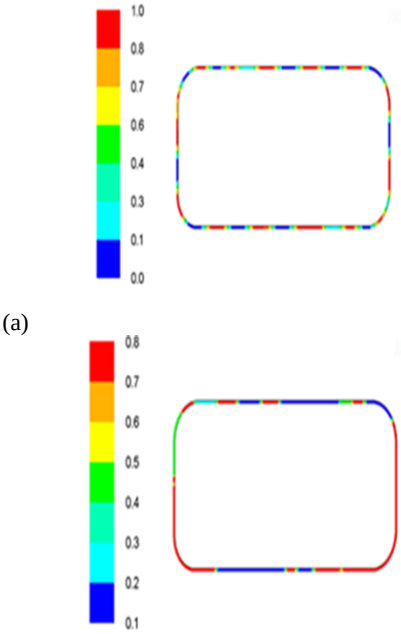

(a)

(b)

Fig. 11. Temperature contours of PHP Vs (a) Al_2 O_3- 0.05 % (b) Al_2 O_3 -0.5 %.

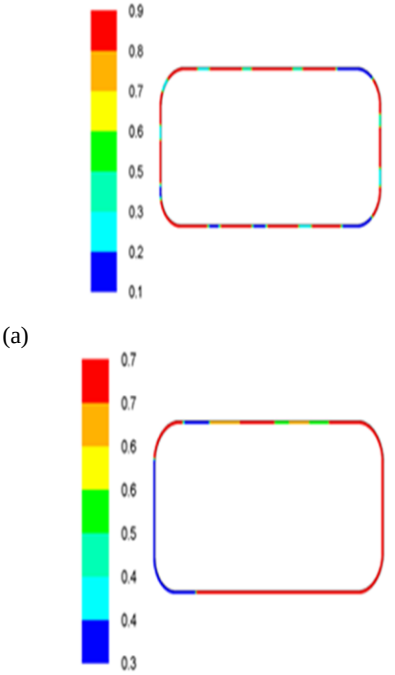

(a)

(b)

Fig. 12. Temperature contours of PHP Vs (a) Al_2 O_3 -1 % (b) water.

not detect very sluggish vapour development and flow imagining in the pipe. When heat input was 12 watts, the inner flow was seen. The rate of bubble development increased as the temperature of the evaporator section increased. The flowing bubble accelerated to catch up with the growth of the bubbles seen in Fig. 11 (a & b). Because of the penetrating boiling of the working fluid, the pressure became unbalanced, resulting in alternating left and

right oscillation. A significant number of bubbles erupted in the cross-section region, and the total fluctuation inside the tube moved to all linked lines. The steady, continuous oscillation is eventually depicted in Fig. 12 (a & b).

4.2 Experimental results compared with Simulation results

Figure 13, shown above, compares experimental and simulated findings. The simulation result was closely related to the experimental data, i.e., in comparison of CFD and experimental results, there will be a 3% variation in temperature differences due to cause for differences in simulation and experimental data listed below.

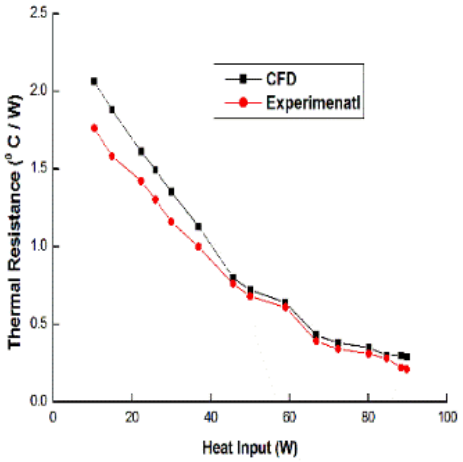

Fig. 13. Experimental Vs Simulation results.

1. The heat loss due to conduction to the condenser and evaporator sections.
2. Convection heat loss occurs in the condenser and evaporator sections.
3. Computational fluid dynamics (CFD) also contains mistakes such as discretization error.

5. CONCLUSION

An experiment was carried out to assess the thermal performance of a single closed loop PHP. $Al_2 O_3$ - DI water nano fluids were employed as working fluids, with different concentrations of aluminium oxide nanoparticles (0.05 %, 0.5 % and 1%). Heat inputs ranged from 10 to 100 watts, and performance characteristics such as thermal resistance, heat transfer coefficient, and thermal conductivity were changed. The study leads to the following conclusions.

1. Compared to DI water, the nanofluids had lower thermal resistance values; nevertheless, as the heat input rises, the performance of the pulsating heat pipe improves.
2. With increasing heat input and nanoparticle concentration, the heat transfer coefficient and thermal conductivity values rise.
3. The average Nusselt number of one volume percent nanofluid was enhanced by 28 % as compare to pure water.
4. Positive increases in thermal conductivity and viscosity for $Al_2 O_3$ nanofluid at volume concentrations of 0.05, 0.5 and 1 %.
5. We determined that the temperature differences between the evaporator and condenser sections during CFD based modeling is 3 % larger than that of experimental results.

ACKNOWLEDGEMENT

The authors acknowledge the facilities used in the research and providing testing facilities at Mechanical Department, JNTUK, Kakinada, India.

REFERENCES

Akachi, H. (1990) .Structure of a micro-heat pipe, US Patent, Patent Number 4921041.

Bai, W., W. Chen, C. Zeng, G. Wu, and X. Chai (2022). Heat transfer and eccentric effect investigation on heat pipe used annular heat exchangers with densely longitudinal fins. *International Journal of Thermal Sciences* 179, 107658.

Dittus, F. W. and L. M. K. Boelter (1930*). Heat Transfer in Automobile Radiators of the Tubular Type*. University of California Publications on Engineering 11, 443 – 461.

Grubisic, L., D. Lacmanovic, M. Palaversa, P. Prebeg and J. Tambaca (2022). An Open-Source Processing Pipeline for Quad-Dominant Mesh Generation for Class-Compliant Ship Structural Analysis. *Journal of Marine Science and Engineering* 10(2).209.

Ji, Y., C. Wilson, H. H. Chen and H. Ma (2011).. Particle Shape Effect on Heat Transfer Performance in an Oscillating Heat Pipe. *Journal of Nanoscale Research Letters* 6 (1), 296.

Karthikeyan, V. K., K. Ramachandran, B. C. Pillai and A. Brusly Solomon (2014). Effect of nanofluids on thermal performance of closed loop pulsating heat pipe. *Experimental Thermal and Fluid Science* 54, 171–178.

Khandekar, S. (2004). *Thermo Hydrodynamics of Pulsating Heat Pipes*. PhD Dissertation, University of Stuttgart, Germany.

Khandekar, S., N. Dollinger and M. Groll (2003). Understanding operational regimes of closed loop PHPs: An experimental study. *Applied Thermal Engineering* 23 (6), 707-719.

Markal, B. and K. Aksoy (2021). The combined effects of filling ratio and inclination angle on thermal performance of a closed loop pulsating heat pipe. *Heat Mass Transfer* 57, 751–763.

Mohammadi, N., M. Mohammadi, and M. B. Shafii (2013). A review of nanofluidic pulsating heat pipes: Suitable choices for thermal management of electronics. *Frontiers in Heat Pipes* (FHP) 3(3), 033001.

Parthasarathi, S., S. Nagarajan and S. Desai (2021). Effect of bend radius and insulation on adiabatic section on the performance of a single closed loop pulsating heat pipe: experimental study and heat transfer correlation. *Heat Mass Transfer* 57, 1871–1892.

Pradeep, G. V. and K. Rama Narasimha (2019). Experimental investigations on the thermal performance of a single closed loop pulsating heat pipe using TiO_2 Nanofluid. *Journal of Heat Transfer* 141(9).

Rahman, M. M. and Z. Saghir (2021). Free convective heat transfer efficiency in Al_2O_3–Cu/water hybrid nanofluid inside a rectotrapezoidal enclosure. *International Journal of Numerical Methods for Heat & Fluid Flow*. 32(1), 196-218.

Rama Narasimha, K., S. N. Sridhara, M. S. Rajagopal and K. N. Seetharamu (2012). Experimental studies on Pulsating Heat Pipe. *International Journal of Mechanical Engineering* 1(1), 46-49.

Rao, C. S., A. Gupta and K. R. Narasimha (2016). Parametric Characterization on the Thermal Performance of a Closed Loop Pulsating Heat Pipe. *Journal of Applied Fluid Mechanic*s 9(2), 615-624.

Sandhya, M., D. Ramasamy, K. Sudhakar, K. Kadirgama and W. S. Harun (2021). Ultrasonication an intensifying tool for preparation of stable nanofluids and study the time influence on distinct properties of graphene nanofluids–A systematic overview. *Ultrasonics sonochemistry* 73, 105479.

Singh, K., D. P. Barai, S. S. Chawhan, B. A. Bhanvase and V. K. Saharan (2021). Synthesis, characterization and heat transfer study of reduced graphene oxide-Al_2O_3 nanocomposite based nanofluids: Investigation on thermal conductivity and rheology. *Materials Today Communications* 26:101986.

Stalin, P. M., T. V. Arjunan, M. M. Matheswaran, P. M. Kumar and N. Sadanandam (2021). Investigations on thermal properties of CeO2/water nanofluids for heat transfer applications. *Materials Today: Proceedings* 47, (19), 6815-6820.

Wang, J., Y. Pan and X. Liu (2021). Investigation on start-up and thermal performance of the single-loop pulsating heat pipe with variable diameter. *International Journal of Heat and Mass Transfer* 180,121811.

Yao, H. L., Guo, H. Liu, X. Wang, H. Chen, Y. Wang and Y. Zhu (2022).Characteristics of phase-change flow and heat transfer in loop thermosyphon:Three-dimension CFD modeling and experimentation. *Case Studies in Thermal Engineering* 35,102070.

Yoon, A. and S. J. Kim (2021).A deep-learning approach for predicting oscillating motion of liquid slugs in a closed-loop pulsating heat pipe. *International Journal of Heat and Mass Transfe*r 181,121860.

Zhang, X., and Y. Zhang (2021).Heat transfer and flow characteristics of Fe3O4-water nanofluids under magnetic excitation. *International Journal of Thermal Sciences* 163, 106826.

Zhou, Y., H. Yang, L. Liu, M. Zhang, Y. Wang, Y. Zhang and B. Zhou (2021). Enhancement of start-up and thermal performance in pulsating heat pipe with GO/water nanofluid. *Powder Technology* 384, 2021, 414-422.